Journal of Alloys and Compounds, *197* (1993) 35–41
JALCOM 637

Investigations of ordered structures in boron-containing Pd_3Mn alloys

Y. Sakamoto, K. Takao, Y. Nagaoka and H. Kida
Department of Materials Science and Engineering, Nagasaki University, Nagasaki 852 (Japan)

T. B. Flanagan
Department of Chemistry, The University of Vermont, Burlington, VT 05405-0125 (USA)

(Received December 8, 1992)

Abstract

The order transitions in Pd_3MnB_y with $y = 0$–0.2 were studied by X-ray, electron diffraction and electrical resistance measurements. The order transition behaviour in low boron content alloys with up to about $y = 0.1$ is substantially the same as that of B-free Pd_3Mn, except that the long-range order ⇄ short-range order transition of the $L1_{2-s}$ structure shifts to a higher temperature with increasing boron content. For high boron content alloys with $y = 0.125$–0.2 quenched from about 1173 K, however, the electron diffraction patterns in some cases exhibited strong superlattice reflections due to the $L1_2$ structure; in other cases the patterns showed weak and diffuse reflections due to superimposed $L1_{2-s}$ and $L1_2$ superlattice reflections. For annealed alloys with high B content, obtained by slow cooling from about 1153 K, the diffraction patterns exhibited mainly two-variant reflections of $L1_{2-s}$ accompanied by the formation of twinned structures.

1. Introduction

The stoichiometric Pd_3Mn alloy is known to form a long-period one-dimensional antiphase domain structure with a domain size $M = 2$, *i.e.* an $L1_{2-s}$-type (Al_3Zr-type) structure, on slowly cooling below its critical temperature $T_c \approx 803$ K [1–7], whereas on rapid quenching into ice-water from high temperatures, *e.g.* about 1193 K, it forms mainly a disordered f.c.c. structure, although electron diffraction shows very faint superlattice reflections of the $L1_{2-s}$ structure.

The electrical resistance behaviour of initially "as-quenched" Pd_3Mn as it is heated from about 300 to 1153 K shows an unusual increase in resistance between 573 and 720 K arising from the onset of ordering to the $L1_{2-s}$-type and has been attributed to the scattering of conduction electrons from the antiphase domain boundaries of the $L1_{2-s}$ structure formed during heating [5–7].

Furthermore, in previous studies [4, 6, 8–11] the present authors have shown that when initially "as-quenched" and initially "ordered (long-range order of $L1_{2-s}$)" alloys are exposed to hydrogen gas at elevated temperature, *e.g.* at 726 K and $p_{H_2} = 5$ MPa, they both transform into another ordered structure, $L1_2$-type (Cu_3Au-type) structure. Conditions of greater hydrogen pressures and high temperatures were shown to be favourable for this hydrogen-induced ordering. The hydrogen-induced $L1_2$ structure is metastable below temperatures of about 650 K even after removal of the dissolved hydrogen [9]. The mechanism of the hydrogen-induced ordering to $L1_2$ has been considered to be related to the lattice expansion caused by the preferential occupation of hydrogen in a special octahedral site of the $L1_{2-s}$ structure.

It is of interest to examine whether or not there is evidence for the existence of similar interstitial-atom-induced ordering in Pd_3Mn containing interstitial boron. Palladium dissolves considerable amounts of boron at high temperature in α-Pd solid solution [12–15]. Although there is no direct evidence that boron occupies octahedral sites in the Pd lattice, the lattice expansion which occurs as a result of the addition is greater than would be expected on the basis of a substitutional alloy, *i.e.* the Pd lattice expands linearly up to B:Pd ≈ 0.22 [12, 13, 15].

The aim of the present research is to examine the effect of boron addition on the order transitions in stoichiometric Pd_3Mn using X-ray, electron microscopy and electrical resistance measurements. The great recent interest in structural intermetallic compounds such as Ni_3Al results partly because their ductility can be increased by B additions [16]. The behaviour of B in

0925-8388/93/$6.00

Pd_3Mn is also of interest because of its relationship to such structurally interesting compounds.

2. Experimental details

The alloys of Pd_3MnB_y used in this study, where $y=0$, 0.05 (B:Mn atom ratio $r_B=0.0125$), 0.1 ($r_B=0.025$), 0.125 ($r_B=0.03125$), 0.15 ($r_B=0.0375$) and 0.2 ($r_B=0.05$), were prepared from palladium (purity 99.98 wt.%), manganese (purity 99.99 wt.%) and boron (purity 99.8 wt.%) by melting under an argon atmosphere in a high frequency induction furnace. After a homogenizing anneal under a vacuum of about 2×10^{-6} Torr at 1123 K for 12 h, the alloy buttons were rolled into specimens about 250–300 μm thick which were used in X-ray diffraction, electron microscopy observations and electrical resistance measurements.

Before measurements of the physical properties, all alloy samples were subjected to the following two kinds of heat treatment.

(1) The samples were quenched rapidly into ice-water after heating at about 1173 K for 10 min in a stream of argon gas, where the samples were wrapped in zirconium foil. These samples will be referred to as "quenched".

(2) The samples were cooled *in vacuo* to room temperature from about 1153 K at a rate of 10 K h^{-1}. These samples will be referred to as "annealed".

For X-ray diffraction studies the sample surfaces were slightly abraded by fine emery paper in order to remove the oxide formed during the heat treatment. They were then electropolished in a solution of perchloric acid and acetic acid (1:4 by volume) to remove the lattice strains introduced by the abrading. X-Ray diffraction with nickel-filtered Cu Kα radiation was carried out at room temperature and the lattice parameters were derived using the Nelson–Riley extrapolation method [17].

The electrical resistance measurements were carried out *in vacuo* by heating initially "as-quenched" alloys and subsequently cooling and then reheating them at temperatures between about 300 and 1153 K. A conventional four-point technique was employed by monitoring with a strip chart recorder. The heating and cooling rates were 10 K h^{-1} instead of the 2 K h^{-1} employed in previous studies [5–7]. The current used was 50 mA.

In order to follow the ordering transitions by electrical resistance–temperature relationships, electron diffraction studies were also carried out on the initially as-quenched samples. Identical alloys were heated and cooled in a separate furnace and then quenched into ice-water from various temperatures during the heating and cooling processes. The samples for electron microscopy observations were jet electropolished in the same electrolyte as described above. Electron diffraction patterns and electron micrographs were taken with a Hitachi H-800 electron microscope.

3. Results and discussion

3.1. X-Ray diffraction studies

The X-ray diffraction line profiles of both quenched and annealed alloys of Pd_3MnB_y with up to $y=0.2$ consisted of reflections due to a single α-f.c.c. palladium phase, except for the quenched alloys with high boron contents, *i.e.* $y=0.15$ and 0.2, where superlattice reflections due to the $L1_2$ structure were also observed. Figure 1 shows the X-ray diffraction line profiles of the quenched Pd_3MnB_y alloys with $y=0.15$ and 0.2. The open circles indicate the $L1_2$ superlattice reflections. The high boron content alloys are thus found to have an equilibrium mixture of $L1_2+\alpha$-Pd as quenched from a high temperature of about 1173 K. As has been observed [1–7] and will be described later, the α-Pd phase corresponds to the short-range-ordered $L1_{2-s}$ structure for the quenched alloys, while the α-Pd in the annealed alloys corresponds to the long-range-ordered $L1_{2-s}$ structure.

Figure 2 shows the lattice parameters of the α-Pd ($L1_{2-s}$) phase determined for both quenched and annealed alloys as a function of boron content together with those of the $L1_2$ structure, and in the same figure the lattice parameters of binary Pd–B solid solution alloys [15] are also given with the same unit of B concentration, *i.e.* Pd_4B_y, for comparison. There is no significant difference in the lattice parameters of the α-Pd phase between quenched and annealed alloys: the lattice parameters increase with increasing boron content up to about Pd_3MnB_y with $y=0.125$, while the lattice parameters of the alloys with more than about $y=0.125$ remain almost constant. The increase in the lattice parameters of the α-Pd phase with increasing

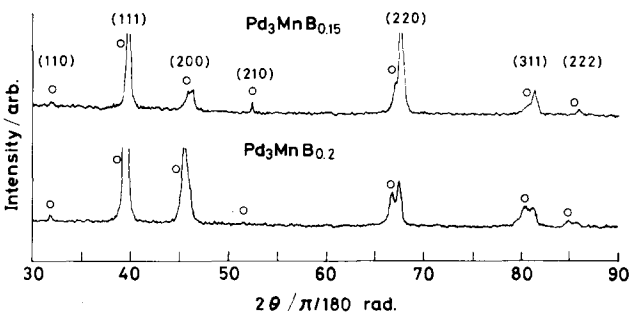

Fig. 1. X-Ray diffraction line profiles of quenched $Pd_3MnB_{0.15}$ and $Pd_3MnB_{0.2}$ alloys at room temperature. The open circles indicate diffraction lines of the $L1_2$ phase. Cu Kα radiation with a nickel filter was used.

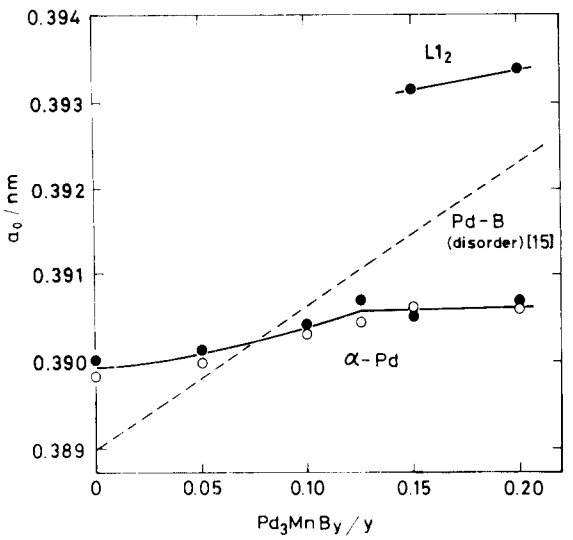

Fig. 2. Room temperature lattice parameters of α-Pd and $L1_2$ phases in Pd_3MnB_y as a function of boron content y: ●, quenched; ○, annealed. The dotted line is the lattice parameter of binary Pd–B solid solution alloys [15] *vs.* B content in Pd_4B_y.

y in Pd_3MnB_y is smaller than that for binary Pd–B solid solution alloys [12, 13, 15]. The lattice parameters of the $L1_2$ phase which coexists with the α-Pd ($L1_{2-s}$) phase at larger values of y are about 0.7% larger than the parameters of the α-Pd ($L1_{2-s}$) phase (Fig. 2). The expansion of the $L1_2$ form with $y=0.2$ is almost the same as that of Pd–B alloys [15]. This supports the notion that the B is in solid solution in these alloys. The anomalous lattice expansion of the α-Pd ($L1_{2-s}$) phase was carefully checked, *e.g.* by examining both samples whose surfaces had been ground by emery paper and those which had been electropolished and by examining different regions of the alloy for possible occlusion of B. The anomalously small expansion seems to be real and may be related to the structure of the $L1_{2-s}$ form and the possible occupation of only the central octahedral interstice which is surrounded by only nearest-neighbour Pd atoms. H occupies this interstice in B-free Pd_3Mn [1]. This interstice surrounded by only Pd atom nearest neighbours occurs in every fourth cell cube, and if these were to be occupied, the expansion would be expected to be very anisotropic in planes perpendicular to the $a_1(c_o)$ axis which is the long dimension of the unit cell. In the case of the $L1_2$ ordered structure the expansion is greater because the Pd-rich interstice appears in every unit cube and the expansion would be isotropic.

3.2. Electron microscopy and electrical resistance measurements

As typical examples, electron diffraction patterns of Pd_3MnB_y alloys with $y=0.05$ and 0.15 which have been subjected to quenching and annealing are shown in Figs. 3 and 4 respectively. The diffraction patterns of low B content alloys with up to $y=0.1$ are substantially the same as those of the B-free Pd_3Mn alloy [1–7]. The patterns of the quenched alloys exhibited mainly weak and diffuse scattering due to short-range order (SRO) of the $L1_{2-s}$ structure, together with fundamental reflections from the α-Pd phase (Fig. 3(a)), while the annealed alloys clearly show the existence of the long-period superlattice of $L1_{2-s}$ (Fig. 3(b)).

In the quenched alloys with higher B content ($y=0.125$–0.2) some regions showed strong reflections due to the $L1_2$ structure (Fig. 4(a)) but other regions showed relatively weak and diffuse reflections which are considered to be a superimposition of the $L1_{2-s}$ and $L1_2$ superlattices (Fig. 4(b)). For the annealed alloys with high B content the diffraction patterns exhibited strong reflections due to the $L1_{2-s}$ structure (Fig. 4(c)), although the patterns in other regions have mainly two-variant reflections (Fig. 4(d)). As the boron content increases, the two-variant reflections emerged as dominant. Figures 5(a)–5(c) show transmission electron micrographs of the annealed alloys of Pd_3MnB_y with $y=0.125$, 0.15 and 0.2 respectively. The charac-

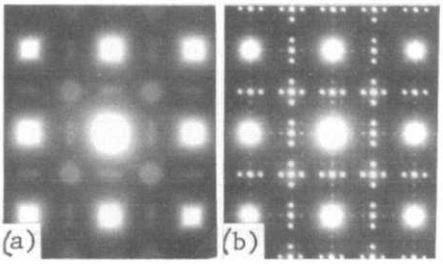

Fig. 3. Electron diffraction patterns with [001] incidence for as-quenched (a) and annealed (b) alloys of Pd_3MnB_y with $y=0.05$.

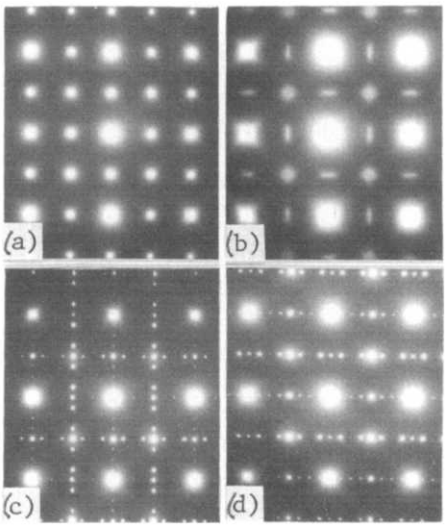

Fig. 4. Electron diffraction patterns with [001] incidence for as-quenched (a), (b) and annealed (c), (d) alloys of Pd_3MnB_y with $y=0.15$.

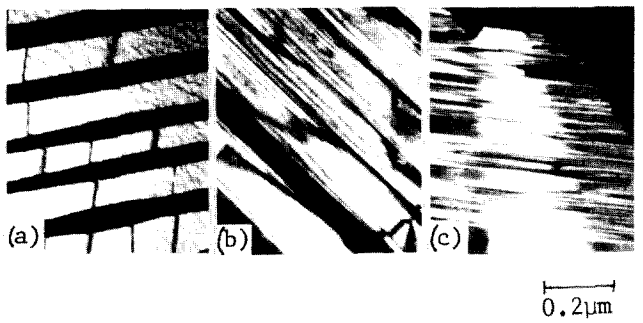

Fig. 5. Transmission electron micrographs of annealed alloys of Pd_3MnB_y with $y=0.125$ (a), dark field image, with (100) reflection, $y=0.15$ (b), dark field image, with (100) reflection and $y=0.2$ (c), dark field image, with (100) reflection.

teristic alignment of the ordered $L1_{2-s}$ domains in the matrix can be observed. The formation of the twinned structure may be due to lattice strains accompanying the $L1_2 \rightarrow L1_{2-s}$ transition during the slow cooling which are relaxed by the formation of a self-accommodating array of twins.

Figure 6 shows electrical resistance *vs.* temperature relationships for a series of Pd_3MnB_y alloys, where R_o in the resistance ratio (R_t/R_o) is the resistance at 1153 K and R_t is the resistance at other temperatures. The arrows with letter labels in the figures indicate temperatures from which samples were quenched into ice-water and examined by electron diffraction. The results of electron diffraction and transmission electron microscopy observations for Pd_3MnB_y alloys during the heating and cooling processes are summarized in Table 1.

It can be seen that the maximum in resistance for the initially quenched alloy of B-free Pd_3Mn which occurs during heating at about 660 K shifts towards higher temperatures with increasing boron content. The maximum in resistance is attributed to the scattering of conduction electrons due to the increase in the periodic antiphase domain boundaries with the onset of ordering to the long-range order (LRO) of $L1_{2-s}$ from the short-range-ordered state and also from the $L1_2$-rich phase for high boron content alloys. It is interesting that the $L1_2$ structure in a quenched alloy of Pd_3MnB_y with $y=0.2$ is maintained even at temperatures up to about 823 K. With further high temperature heating, the resistance decreases first with coarsening of the $L1_{2-s}$ ordered domains; however, for the alloy with $y=0.2$ the resistance remains almost constant. Thereafter there is again an appearance of a maximum in resistance at about 940–1000 K. It is evident from electron diffraction studies that the second maximum in resistance corresponds to the reverse transition $L1_{2-s} \rightarrow L1_2$. Thus the increase in resistance is also attributed to the scattering of conduction electrons due to the disintegration of the periodic antiphase

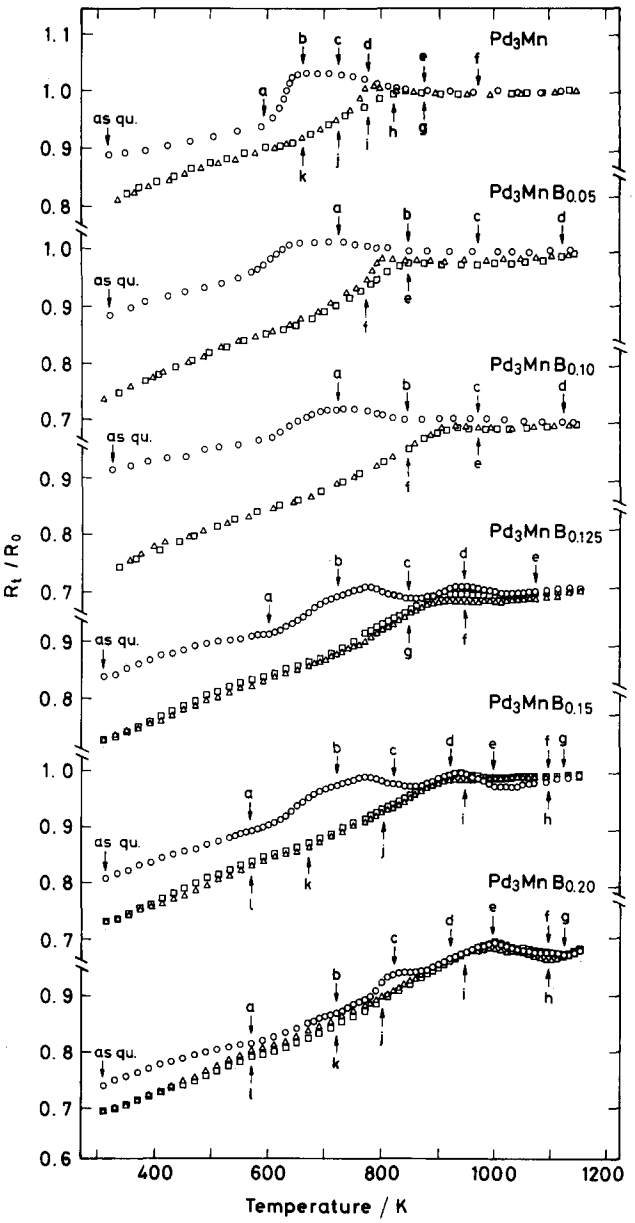

Fig. 6. Electrical resistance ratio R_t/R_o *vs.* temperature for initially quenched Pd_3MnB_y alloys as they are heated (○), subsequently cooled (△) and then reheated (□). The heating and cooling rates were 10 K h^{-1}.

domain boundaries from the onset of transition to the $L1_2$ structure from the long-range order of $L1_{2-s}$.

Figures 7(a)–7(g) show electron diffraction patterns and transmission electron micrographs of Pd_3MnB_y alloys with $y=0.2$ quenched from temperatures of 823 K (a), (b), 923 K (c), (d) and 998 K (e)–(g) during the heating process. The diffraction patterns for the sample quenched from 823 K, *i.e.* directly before transforming to $L1_{2-s}$ from $L1_2$, produce ⟨100⟩ streaks through the origin of reciprocal space (Fig. 7(a)). At 923 K the reflections due to the retransformed $L1_{2-s}$ are clearly observed (Fig. 7(c)) and at 998 K some

TABLE 1. Summary of electron diffraction results for Pd_3MnB_y alloys with $y=0$–0.2 during heating and cooling processes: (s), (m), (w) and (d) refer to strong, medium and weak reflections and diffuse scattering respectively in the electron diffraction patterns; * indicates two-variant reflections of $L1_{2-s}$; "as-quenched" indicates that samples were quenched rapidly into ice-water after heating at about 1173 K for 10 min in a stream of argon gas; "annealed" indicates that samples were cooled *in vacuo* to room temperature from about 1153 K at a rate of 10 K h^{-1}

Alloy	Heating process		Cooling process	
	Quenching temperature (K)	Crystal structure	Quenching temperature (K)	Crystal structure
Pd_3Mn	As quenched	$L1_{2-s}$(w, d)	g 876	$L1_{2-s}$(d)
	a 592	$L1_{2-s}$(d)	h 823	$L1_{2-s}$(d)
	b 663	$L1_{2-s}$(m)	i 778	$L1_{2-s}$(s)
	c 726	$L1_{2-s}$(s)	j 726	$L1_{2-s}$(s)
	d 778	$L1_{2-s}$(s)	k 663	$L1_{2-s}$(s)
	e 876	$L1_{2-s}$(d)	Annealed	$L1_{2-s}$(s)
	f 971	$L1_{2-s}$(d)		
$Pd_3MnB_{0.05}$	As quenched	$L1_{2-s}$(d)	e 848	$L1_{2-s}$(d)
	a 723	$L1_{2-s}$(m)	f 773	$L1_{2-s}$(s)
	b 848	$L1_{2-s}$(s)	Annealed	$L1_{2-s}$(s)
	c 973	$L1_{2-s}$(d)		
	d 1123	$L1_{2-s}$(d)		
$Pd_3MnB_{0.1}$	As quenched	$L1_{2-s}$(d)	e 973	$L1_{2-s}$(d)
	a 723	$L1_{2-s}$(d)	f 848	$L1_{2-s}$(s)*
	b 848	$L1_{2-s}$(s)	Annealed	$L1_{2-s}$(s)*
	c 973	$L1_{2-s}$(m)* ~ $L1_{2-s}$(d)		
	d 1123	$L1_{2-s}$(d)		
$Pd_3MnB_{0.125}$	As quenched	$L1_{2-s}$(d) + $L1_2$(d)	f 948	$L1_{2-s}$(m) + $L1_2$(d)
	a 603	$L1_{2-s}$(d) + $L1_2$(d)	g 848	$L1_{2-s}$(s)*
	b 723	$L1_{2-s}$(d)	Annealed	$L1_{2-s}$(s)*
	c 848	$L1_{2-s}$(s)		
	d 948	$L1_{2-s}$(s)*		
	e 1073	$L1_2$(d) + $L1_{2-s}$(d)		
$Pd_3MnB_{0.15}$	As quenched	$L1_2$(s) + ($L1_2$(d) + $L1_{2-s}$(d))	h 1098	$L1_2$(s) + ($L1_2$(d) + $L1_{2-s}$(d))
	a 573	$L1_2$(m) + ($L1_2$(d) + $L1_{2-s}$(d))	i 948	$L1_{2-s}$(s) + ($L1_2$(m) + $L1_{2-s}$(d))
	b 723	$L1_{2-s}$(d) + $L1_2$(d)	j 803	$L1_{2-s}$(s)*
	c 823	$L1_{2-s}$(s)	k 673	$L1_{2-s}$(s)*
	d 923	$L1_{2-s}$(s)	l 573	$L1_{2-s}$(s)*
	e 998	$L1_{2-s}$(s)* + $L1_2$(d)	Annealed	$L1_{2-s}$(s)*
	f 1098	$L1_2$(m) + ($L1_{2-s}$(d) + $L1_2$(d))		
	g 1123	$L1_2$(s) + ($L1_2$(d) + $L1_{2-s}$(d))		
$Pd_3MnB_{0.2}$	As quenched	$L1_2$(s) + ($L1_2$(w) + $L1_{2-s}$(w))	h 1098	$L1_2$(s) + ($L1_{2-s}$(w) + $L1_2$(w))
	a 573	$L1_2$(s) + $L1_2$(w)	i 948	$L1_{2-s}$(s)*
	b 723	$L1_2$(s) + $L1_2$(w)	j 803	$L1_{2-s}$(s)*
	c 823	$L1_2$(m)	k 723	$L1_{2-s}$(s)*
	d 923	$L1_{2-s}$(s)	l 573	$L1_{2-s}$(s)*
	e 998	$L1_2$(s) + $L1_{2-s}$(s)*	Annealed	$L1_{2-s}$(s)*
	f 1098	$L1_2$(s) + ($L1_{2-s}$(w) + $L1_2$(w))		
	g 1123	$L1_2$(s) + ($L1_{2-s}$(w) + $L1_2$(w))		

regions show similar two-variant reflections due to the remaining $L1_{2-s}$ (Fig. 7(e)) just as observed in the annealed samples described above, but other regions in the sample show the reflections due to the retransformed $L1_2$ (Fig. 7(f)). At higher temperatures of 1098 and 1123 K the diffraction patterns were almost the

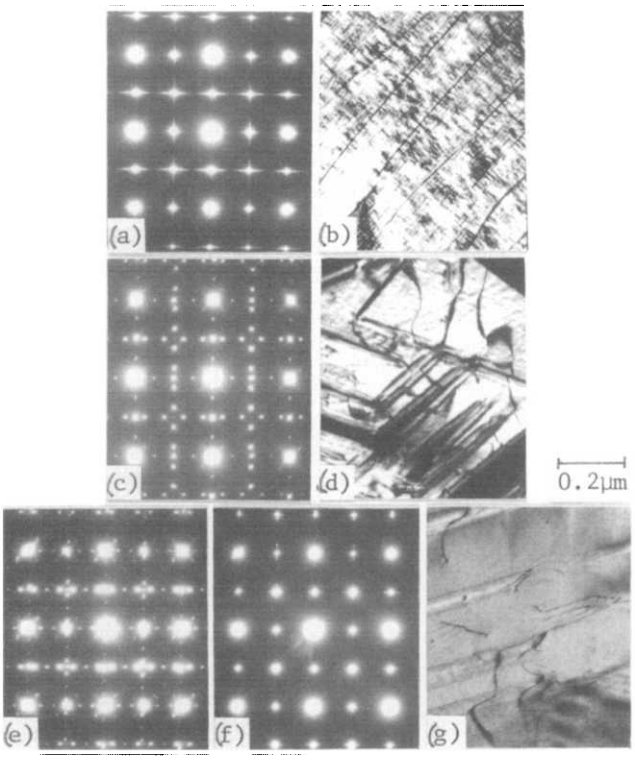

Fig. 7. Electron diffraction patterns with [001] incidence and transmission electron micrographs of Pd_3MnB_y alloys with $y=0.2$ quenched from temperatures of 823 K (a), (b), 923 K (c), (d) and 998 K (e)–(g) during heating process: (b), dark field image, with (100) reflection; (d), dark field image, with (110) reflection; (g), bright field image.

same as those of the "as-quenched" alloys, *i.e.* some regions have strong reflections due to the $L1_2$ structure and in others weak and diffuse reflections from both $L1_{2-s}$ and $L1_2$ are observed.

As can be seen from the subsequent cooling and reheating of the B-free alloy (Fig. 6), the LRO⇄SRO transition of the $L1_{2-s}$ structure observed at about 800 K shifts towards higher temperatures with increasing boron content up to about $y=0.1$, while for the alloys with more than $y=0.1$ the transition temperature remains almost constant, where the transition corresponds to LRO $L1_{2-s}\rightleftarrows L1_2+(L1_{2-s}+L1_2)$ rather than to LRO⇄SRO of $L1_{2-s}$.

Figures 8(a)–8(f) show electron diffraction patterns and transmission electron micrographs of Pd_3MnB_y alloys with $y=0.2$ quenched from temperatures of 1098 and 948 K during the cooling process. At 1098 K during cooling, some regions show strong reflections due to $L1_2$ (Fig. 8(a)) and others show reflections due to superimposition of the $L1_{2-s}$ and $L1_2$ superlattices (Fig. 8(b)). However, at 948 K during cooling, the diffraction patterns exhibit the two-variant reflections due to the transformed $L1_{2-s}$ structure (Fig. 8(d)). It can be concluded that at higher temperatures the $L1_2$ structure is more stable and at lower temperatures the $L1_{2-s}$ structure is stable and the stability of $L1_{2-s}$ also increases with increasing B content.

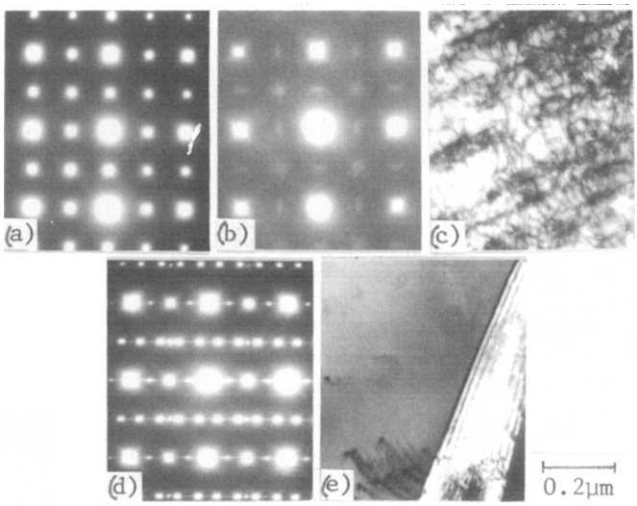

Fig. 8. Electron diffraction patterns with [001] incidence and transmission electron micrographs of Pd_3MnB_y alloys with $y=0.2$ quenched from temperatures of 1098 K (a)–(c) and 948 K (d), (e) during cooling process: (c), bright field image; (e), dark field image, with (110) reflection.

The mechanism for the reverse transition $L1_{2-s}\rightarrow L1_2$ in Pd_3Mn alloys containing boron during heating is unknown. In the hydrogen-induced ordering from $L1_{2-s}$ to $L1_2$ [4–11] it has been proposed that it may be initiated at the periodic one-dimensional antiphase boundaries in which a step shift $(\vec{a}_2+\vec{a}_3)/2$ is introduced at every two-cell boundary by the stress induced by the preferential occupation of the Pd-rich interstices [11]. A similar mechanism may be operative here, but in this case the occupation of these interstices by B assists the shift. A B content of $y=0.125$ for the formation of the $L1_2$ structure corresponds to a B-to-metal atom ratio $r_B=0.031$; this value is about 25% of the octahedral interstices with six Pd atoms as nearest neighbours in the $L1_{2-s}$ structure, because the interstices in the one-dimensional antiphase domain structure of the $L1_{2-s}$ type are 0.125 per metal atom.

The formation of many twinned structures during the $L1_2\rightarrow L1_{2-s}$ transition by the slow cooling process may be attributed to lattice strains from the $L1_{2-s}$ lattice contraction along the long-period direction which are relaxed by the formation of a self-accommodating array of twins.

The presence of interstitial B has been shown to play a role in the ordering of Pd_3Mn. This may prove to be relevant to the behaviour of structural intermetallic compounds containing B [16].

Acknowledgments

The authors would like to express their gratitude to Tanaka Kikinzoku K. K. for the loan of the palladium

metal. T. B. F. wishes to thank the National Science Foundation for financial support.

References

1 P.-J. Ahlzén, Y. Andersson, R. Tellgren, D. Rodic, T. B. Flanagan and Y. Sakamoto, *Z. Phys. Chem. N. F., 163* (1989) 213.
2 D. Watanabe, *Trans. JIM, 3* (1962) 234.
3 H. Sato and R. S. Toth, *Phys. Rev., 139* (1965) A1581.
4 T. B. Flanagan, A. P. Craft, T. Kuji, K. Baba and Y. Sakamoto, *Scr. Metall., 20* (1986) 1745.
5 K. Baba, Y. Sakamoto, T. B. Flanagan, T. Kuji and A. P. Craft, *Scr. Metall., 21* (1987) 299.
6 T. B. Flanagan, A. P. Craft, Y. Niki, K. Baba and Y. Sakamoto, *J. Alloys Comp., 184* (1992) 69.
7 K. Baba, Y. Niki, Y. Sakamoto and T. B. Flanagan, *J. Alloys Comp., 179* (1992) 321.
8 K. Baba, Y. Niki, Y. Sakamoto, T. B. Flanagan and A. P. Craft, *Scr. Metall., 21* (1987) 1147.
9 K. Baba, Y. Niki, Y. Sakamoto, A. P. Craft and T. B. Flanagan, *J. Mater. Sci. Lett., 7* (1988) 1160.
10 K. Baba, Y. Niki, Y. Sakamoto and T. B. Flanagan, *J. Less-Common Met., 172–174* (1991) 246.
11 Y. Sakamoto, K. Baba, Y. Niki, Y. Ishibashi and T. B. Flanagan, *J. Alloys Comp., 184* (1992) 57.
12 R. Burch and F. A. Lewis, *Trans. Faraday Soc., 66* (1970) 727.
13 H. Brodowsky and H.-J. Schaller, *Ber. Bunsenges. Phys. Chem., 80* (1976) 656.
14 R. A. Alqasmi, H. Brodowsky and H.-J. Schaller, *Z. Metallkd., 73* (1982) 331.
15 Y. Sakamoto, K. Baba and T. B. Flanagan, *Z. Phys. Chem. N. F., 158* (1988) 223.
16 C. T. Liu, C. L. White and J. A. Horton, *Acta Metall., 33* (1985) 213.
17 J. P. Nelson and D. P. Riley, *Proc. Phys. Soc., 9* (1945) 160.